NJC

New Journal of Chemistry

A journal for new directions in chemistry

Accepted Manuscript

This article can be cited before page numbers have been issued, to do this please use: Z. Xiao, Y. Zhou, W. Xu, T. J. Prior, B. Bian, C. Redshaw, Z. Tao and X. Xiao, *New J. Chem.*, 2019, DOI: 10.1039/C9NJ03254A.

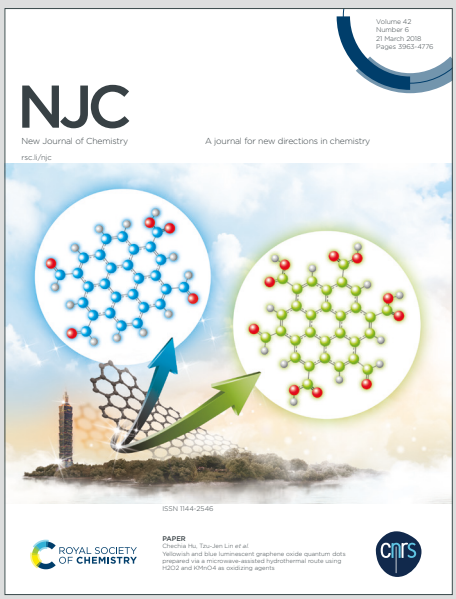

View Article Online
DOI: 10.1039/C9NJ03254A

Study of the host-guest interaction between *N*,*N*$^{/}$-bis[4-(dimethylaminophenyl)methyl]butane-1,4-diamine and the cucuribit[*n*]urils (n = 6, 7)

Zhiyou Xiao,[a] Yang Zhou,[b] Weitao Xu,[c] Timothy J. Prior,[d] Bing Bian,[e] Carl Redshaw,[d]* Zhu Tao[c] and Xin Xiao,[c]*

[a] *School of Chemical Engineering, Guizhou Institute of Technology, Guiyang550003, China*

[b]*College of Chemistry, Chemical Engineering and Materials Science,Shandong Normal University, Jinan 250014, China*

[c]*Key Laboratory of Macrocyclic and Supramolecular Chemistry of Guizhou Province, Guizhou University, Guiyang 550025, China*

[d] *Department of Chemistry & Biochemistry, University of Hull, Hull HU6 7RX, U.K.*

[e]*College of Chemistry and Environmental Engineering, Shandong University of Science and Technology, Qingdao 266590, China.*

Abstract: The interaction between the cucuribit[*n*]urils (Q[*n*]), where n = 6 or 7, and the guest *N*,*N*$^{/}$-bis[4-(dimethylaminophenyl)methyl]butane-1,4-diamine (**G**) has been studied in aqueous solution by ^{1}H NMR spectroscopy, electronic absorption spectroscopy and Isothermal Titration Calorimetry (ITC). In the case of Q[6], a 1:1 host-guest complex is favoured with on end of **G** initially embedded in the Q[6], although over time (48h), the Q[6] shuttles along the chain such that it resides over the centre of **G**. For Q[7], a 2:1 host-guest complex is formed with the aromatic groups at each end of **G** buried in a Q[7] cavity. The molecular structure of the inclusion complex having composition overall composition of Q[6].**G**H_2.2Cl.14H_2O has been determined, and clearly shows the insertion of the guest molecule with the host Q[6] and it is localised therein by two N-H···O hydrogen bonds.

View Article Online
DOI: 10.1039/C9NJ03254A

Keywords: cucuribit[*n*]urils; host-guest; *N*,*N*′-bis[4-(dimethylaminophenyl)methyl]butane-1,4-diamine; molecular structure.

Introduction

Host-guest chemistry continues to be an area of immense interest given its potential for a range of applications.[1] Of the many hosts available, the cucurbit[*n*]uril (Q[*n*]) family is a relatively new arrival, whose chemistry continues to expand at a pace, and whose excellent host-guest binding ability and emerging derivative chemistry is opening up new avenues for their potential application.[2] For example, very recently, systems incorporating Q[7] have recently been combined with quantum dots and employed as sensors for small molecules.[3] As part of an on-going programme investigating the host-guest properties of Q[*n*]s, we have reported Q[6] and Q[7] inclusion complexes involving drug-like molecules such as Adefovir, as well as a number of charged guests.[4] Additionally, for a Q[8]-based system, we have observed how it is possible for the alkyl chains of a guest such as *N*,*N*′-bis(4-dimethylaminobenzyl)-dodecane-1,12-diamine to adopt coiled conformations possessing different chirality.[5] Herein, we investigate the use of *N*,*N*′-bis[4-(dimethylaminophenyl)methyl]butane-1,4-diamine, which can also be named *N*,*N*′-bis[4-(dimethylamino)benzyl]-1,4-butanediamine, **G** and its host-guest behavior in the presence of Q[6] or Q[7]. We note that little is known about the possible applications of guest **G**, although it does appear in the patent literature relating to treating diseases and conditions.[6]

View Article Online
DOI: 10.1039/C9NJ03254A

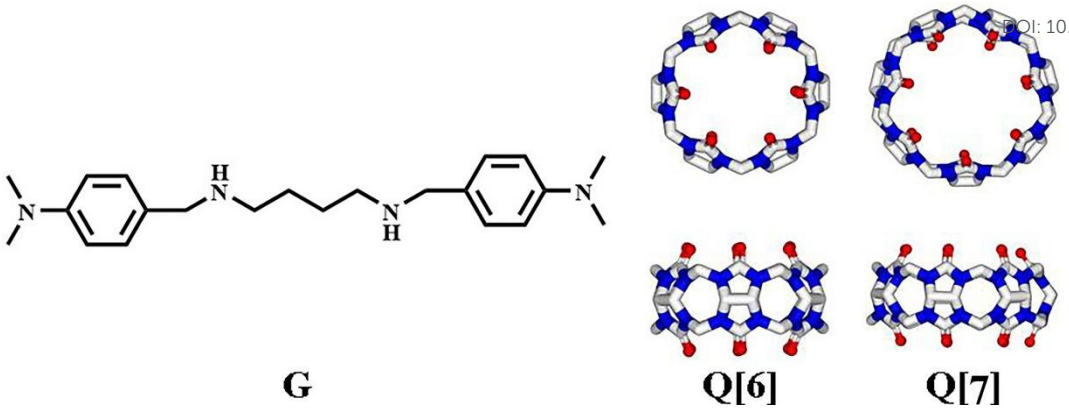

Chart 1. Guest **G** and Q[6] and Q[7].

Results and Discussion

The binding interactions between the guest **G** and Q[6] and Q[7] can be conveniently monitored using ^{1}H NMR spectroscopic data recorded in neutral D_2O solution. Figure 1 shows the changes observed in the spectrum of **G** as progressively larger amounts (0 to 1.949 equiv.) of Q[6] are added to the solution. It is evident that on addition of 0.186 equiv. of Q[6], there are significant chemical shift changes associated with about half of the protons present. Specifically, the aromatic protons b and c, together with the methylene group d are shifted somewhat up-field, whereas a, e and f experience splitting and down-field shifts. This is consistent with encapsulation of one of the aryl groups as depicted in the cartoon shown top right in figure 1. [4f] The situation for e and f is further enhanced upon the addition of more than one equivalent of G (see spectra G and H below).

View Article Online
DOI: 10.1039/C9NJ03254A

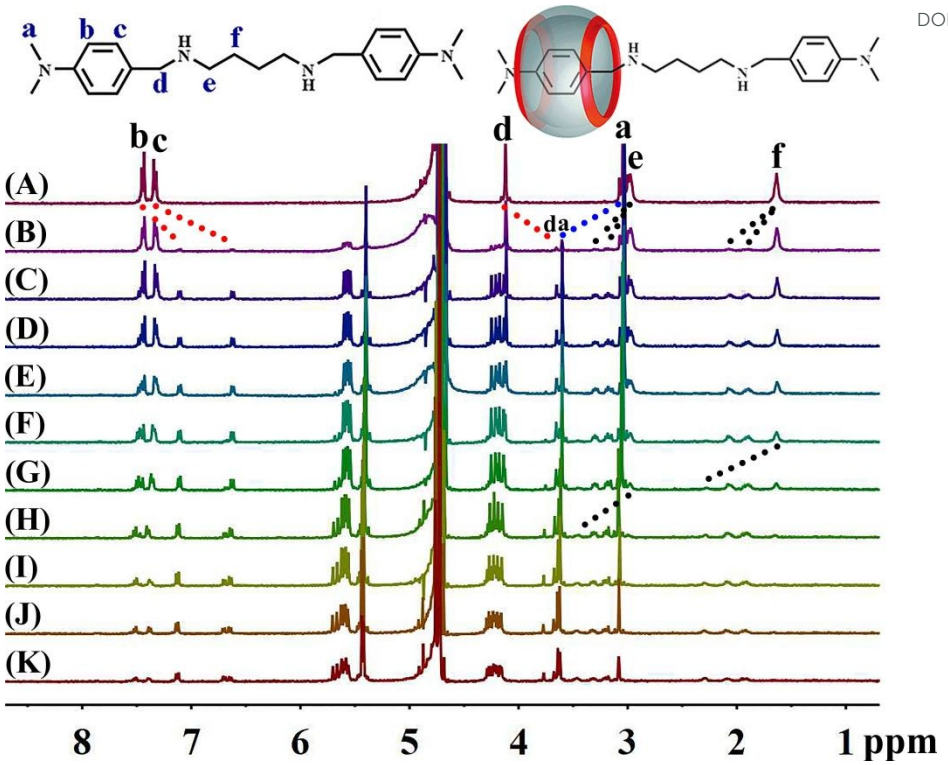

Figure 1. Interaction of **G** and Q[6] (20 ℃): (A) ^{1}H NMR spectra (400 MHz, D_2O) of **G** (*ca*. 2 mM) in the absence of Q[6]; (B) in the presence of 0.186 equiv. of Q[6]; (C) in the presence of 0.424 equiv. of Q[6]; (D) in the presence of 0.568 equiv. of Q[6]; (E) in the presence of 0.800 equiv. of Q[6]; (F) in the presence of 0.846 equiv. of Q[6]; (G) in the presence of 1.058 equiv. of Q[6]; (H) in the presence of 1.377 equiv. of Q[6]; (I) in the presence of 1.597 equiv. of Q[6]; (J) in the presence of 1.701 equiv. of Q[6]; (K) in the presence of 1.949 equiv. of Q[6].

Interestingly, on extending the time to 48h, in the presence of almost 2 equiv. of Q[6], there is a change in the behavior of the system, see figure 2. In particular, the ^{1}H NMR data are consistent with the Q[6] having shuttled along to the centre of **G** resulting in down-field shifts for b – d and up-field shifts for e and f consistent with the cartoon depicted above C below.

View Article Online
DOI: 10.1039/C9NJ03254A

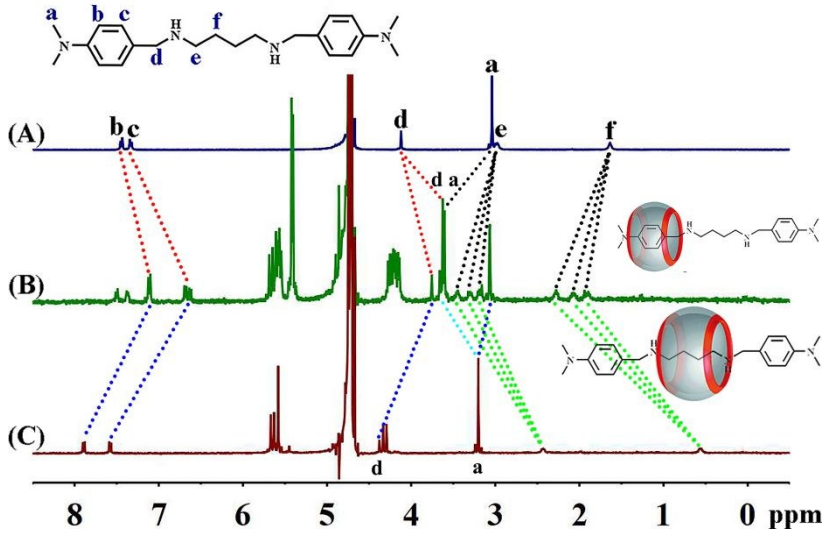

Figure 2. (A) Interaction of **G** and Q[6] (20 ℃, D_2O): ^1H NMR spectra of **G** (*ca*. 2 mM) in the absence of Q[6]; (B) in the presence of 1.949 equiv. of Q[6] (B) at 10 min.; (C) in the presence of 1.949 equiv. of Q[6] after 48h.

On changing the pH to 1.0, the situation is similar with encapsulation of one end of **G** by the Q[6], see figure 3. Again, on prolonged standing (48h), there is a shuttling of the Q[6] to the centre of **G** (see figure 4). Furthermore, a series of variable temperature experiments have also been carried. A thermodynamic arrangement was found to occur between Q[6] and guest **G**. The formation of the Q[6]@**G** complex could be conveniently monitored by ^1H NMR in D_2O at 20℃, 40℃, 60℃ and 80℃, respectively. As shown in Figure S1B, the aryl groups were encapsulated into the cavity of Q[6] at 20℃. On gradually increasing the temperature (from 40℃ to 80℃), obvious differences for the host–guest inclusion complex of Q[6]@**G** were seen in the ^1H NMR spectra in D_2O at 20℃. In particular, the methylene protons d, e and f are shifted somewhat up-field, indicating that the alkyl chain is accommodated in the cavity of Q[6], which is consistent with the observations on extending the time over 48h.

View Article Online
DOI: 10.1039/C9NJ03254A

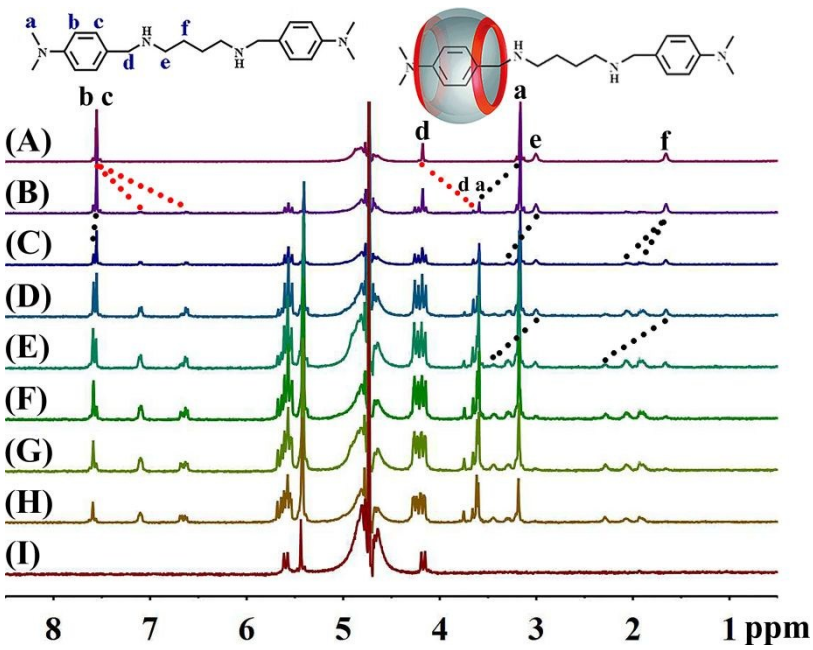

Figure 3. Interaction of **G** and Q[6] (20 ℃): (A) ^{1}H NMR spectra (400 MHz, DCl, pH=1) of **G** (*ca*. 2 mM) in the absence of Q[6]; (B) in the presence of 0.246 equiv. of Q[6]; (C) in the presence of 0.604 equiv. of Q[6]; (D) in the presence of 0.937 equiv. of Q[6]; (E) in the presence of 1.149 equiv. of Q[6]; (F) in the presence of 1.408 equiv. of Q[6]; (G) in the presence of 1.578 equiv. of Q[6]; (H) in the presence of 1.955 equiv. of Q[6]; (I) and with neat Q[6].

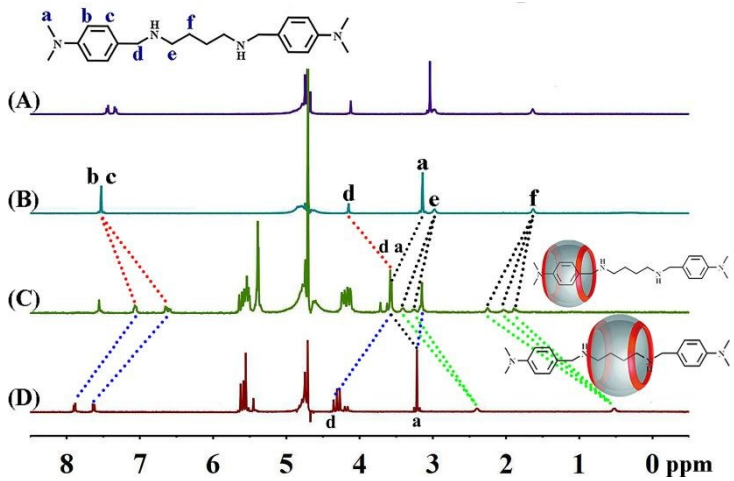

Figure 4. Interaction of **G** and Q[6] (20 ℃): (A) ^{1}H NMR spectra (400 MHz, D_2O) of **G** (*ca*. 2 mM) in the absence of Q[6]; (B) ^{1}H NMR spectra (400 MHz, DCl, pD=1) of **G** (*ca*. 2 mM) in the absence of Q[6]; (C) in the presence of 1.755 equiv. of Q[6]; (D) in the presence of 1.955 equiv. of Q[6] after 48h.

In the case of Q[7] (see figure 5), up-field shifts are initially noted for the protons b – d, and down-field shifts for protons e and f. At 1.53 equiv. of Q[7], there are further shifts associated with the protons d and f, and thereafter further additions of Q[7] lead to little change. These

View Article Online
DOI: 10.1039/C9NJ03254A

results are consistent with two Q[7] molecules encapsulating the aromatic groups at end of the guest G. In contrast to the use of Q[6], there is no change in the mode of encapsulation over time for 2Q[7]@G.

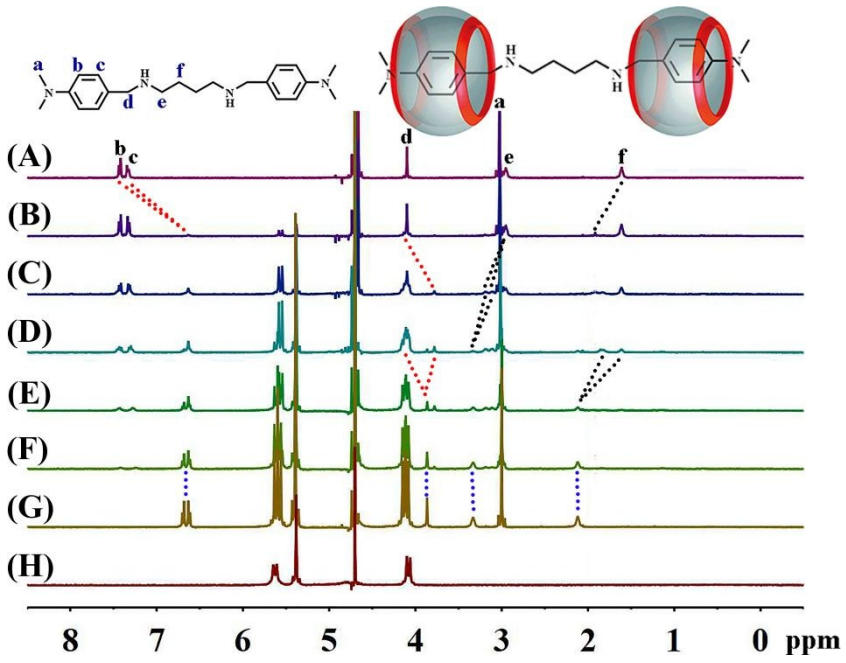

Figure 5. Interaction of **G** and Q[7] (20 ℃): (A) ^{1}H NMR spectra (400 MHz, D_2O) of **G** (*ca*. 2 mM) in the absence of Q[7]; (B) in the presence of 0.102 equiv. of Q[7]; (C) in the presence of 0.502 equiv. of Q[7]; (D) in the presence of 0.959 equiv. of Q[7]; (E) in the presence of 1.530 equiv. of Q[7]; (F) in the presence of 1.981 equiv. of Q[7]; (G) in the presence of 2.272 equiv. of Q[7]; (H) and with neat Q[7].

UV spectroscopy

To further understand the binding of **G** to Q[6] and Q[7], we also investigated, by UV-vis spectrometry, the interactions between Q[6] and Q[7] and G. In Figure 6, the UV spectra were obtained using aqueous solutions containing a fixed concentration of **G** and variable concentrations of either Q[6]. Typically, Q[6] does not exhibit absorbance for $\lambda > 210$ nm, whilst the guest G exhibits a maximum absorbance at 258 nm. Herein, the absorption band of the guest **G** exhibits a progressive decrease in absorbance with a red shift from 258 to 263 nm as the Q[6]/G ratio is gradually increased.

View Article Online
DOI: 10.1039/C9NJ03254A

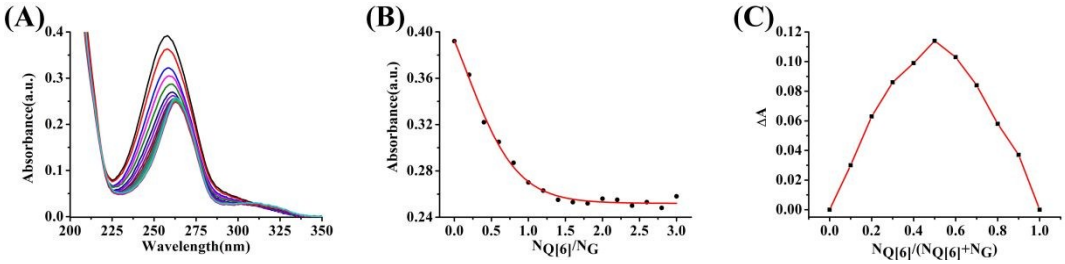

Figure 6. (Colour online) (A) Fluorescence absorption of **G** (2×10^{-5} mol L^{-1}) upon addition of increasing amounts (0, 0.2, 0.4……2.6, 2.8, 3.0 equiv.) of Q[6]; (B) the concentrations and absorbance *vs*. $N_{Q[6]}/N_G$ plots; (C) the corresponding $\Delta A–N_{Q[6]}/(N_{Q[6]} + N_G)$ curves.

The situation for Q[7]/G is shown in figure 7 and reveals somewhat different observations as the Q[7]/G ratio is gradually increased. In this case, upon addition of Q[7], the complexation of G afforded a decrease in the absorption until a 2:1 host-guest ratio was achieved. These observations suggest the formation of a 2:1 host-guest complex between Q[7] and G, and the formation a dumbbell-shaped pseudorotaxane supramolecular structure. Furthermore, the stoichiometry was confirmed by a Job's plot (figure 7 C). The UV data for the molar ratio of host Q[7] to the guest ($N_{Q[7]}/N_G$) fitted a 2:1 binding model.

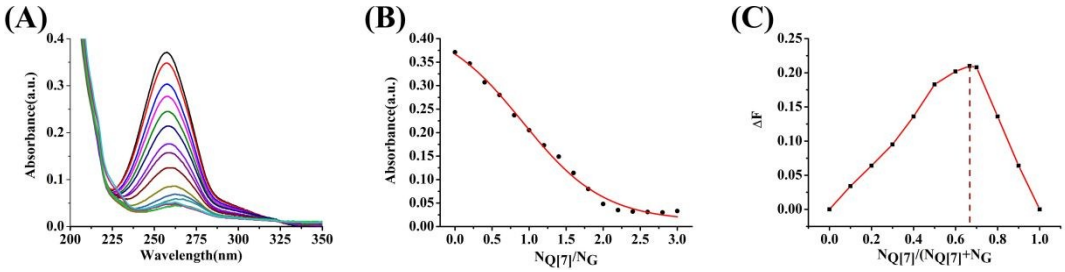

Figure 7. (Colour online) (A) Fluorescence absorption of **G** (2×10^{-5} mol L^{-1}) upon addition of increasing amounts (0, 0.2, 0.4……2.6, 2.8, 3.0 equiv.) of Q[7]; (B) the concentrations and absorbance *vs*. $N_{Q[7]}/N_G$ plots; (C) the corresponding $\Delta A–N_{Q[7]}/(N_{Q[7]} + N_G)$ curves.

ITC analysis

In order to obtain quantitative data on the host-guest complexations observed herein, we have

View Article Online
DOI: 10.1039/C9NJ03254A

conducted ITC measurements. A solution of G was consecutively injected into a solution of Q[6] (or Q[7]) at 25 °C to record the exothermic binding isotherm. The results are depicted in figures S2 and S3, and table 1, and affords the association constants K_a = 2.615×10^4 M^{-1} for Q[6] and 3.666×10^6 M^{-1} for Q[7] were determined from this data. These high binding constants, particularly for the Q[7] system, indicate the formation of stable inclusion complexes in aqueous solution. The large negative enthalpy values indicate that this process is driven by a favourable enthalpy change.

Table 1. Data obtained from ITC experiments.

Host-Guest	K_a /(M^{-1})	ΔH^o /(kJ·mol^{-1})	$T\Delta S^o$ /(kJ·mol^{-1})
Q[6]@G	(2.615 ± 0.06)×10^4	-100.00 ± 0.05	-73.48 ± 0.09
Q[7]@G	(6.741 ± 0.07)×10^9	-14.634 ± 0.08	-2.83 ± 0.11

X-ray crystallography

A crystal was selected from the reaction of Q[6] with *N*,*N*′-bis[4-(dimethylaminophenyl)methyl]butane-1,4-diamine in 3 M HCl. The molecular structure is shown in figure 8 and figure 9 (alternative views are provided in figure S4, ESI); crystallographic data is presented in table 2. The structure clearly shows the insertion of the guest molecule with the host Q[6] and it is localised therein by two N-H···O hydrogen bonds. The structure is centrosymmetric and crystallises with one half of the guest and one half of the host molecule in the asymmetric unit. The whole complex is generated by the symmetry operator 1.5−*x*, 0.5−*y*, 0.5−*z* and this arrangement is centrosymmetric and has minor disorder of the guest molecule. Within the crystal structure the primary amine at each of the end of the guest is protonated. Each of the two N−H bonds form a hydrogen bond to the carbonyl on the rim of the Q[6] as follows: N(21)-H(21A)···O(4)^i and N(21)-H(21B)···O(6)^i with N…O distances of

View Article Online
DOI: 10.1039/C9NJ03254A

2.819(4) and 2.955(4) Å respectively. It was not possible to locate the molecules outside the complex because these were hugely disordered. The electron density corresponding to these regions was modelled using the SQUEEZE routine and this gives and overall composition of Q[6].GH_2.2Cl.14H_2O.

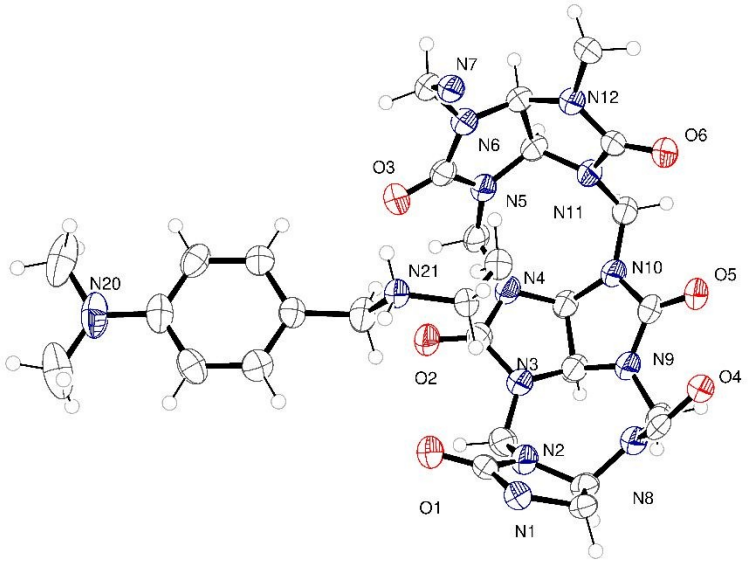

Figure 8. ORTEP plot of the asymmetric unit of **1** with atoms drawn as 50 % probability ellipsoids. For clarity the minor disorder is not shown.

View Article Online
DOI: 10.1039/C9NJ03254A

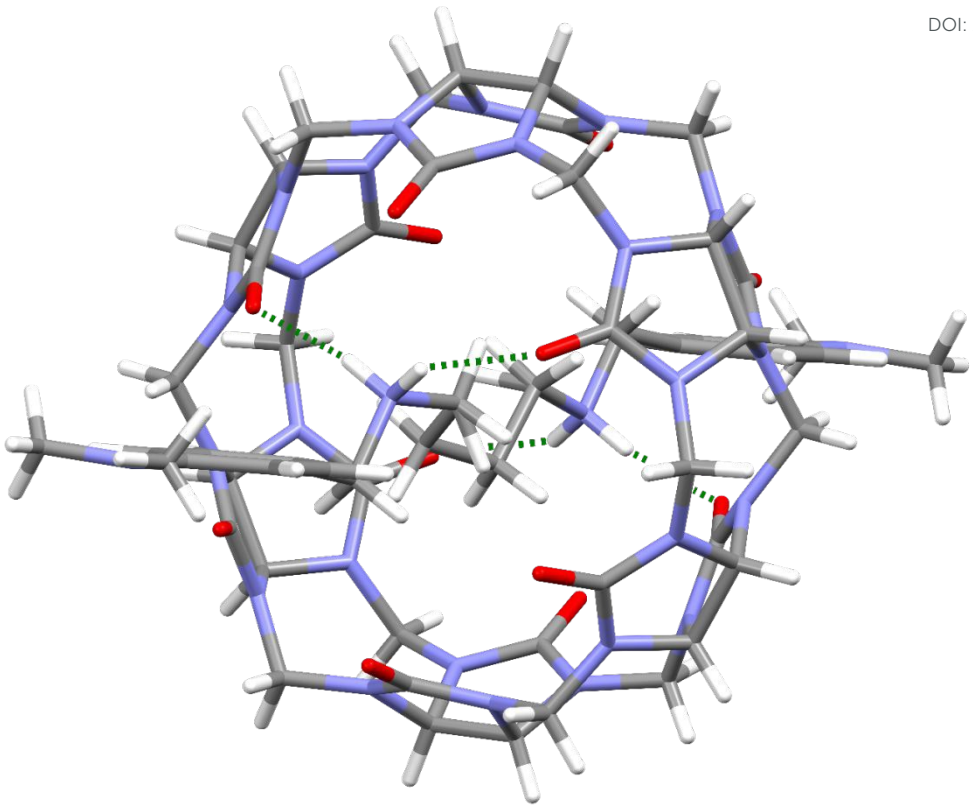

Figure 9. Host guest complex sustained by hydrogen bonding (shown as green dashed lines)

Table 2. Crystal data and structure refinement of **1**.

Empirical formula	$C_{58}H_{72}N_{28}O_{12}$	
Formula weight	1353.43	
Temperature	293(2) K	
Wavelength	0.71073 Å	
Crystal system	Monoclinic	
Space group	I 2/a	
Unit cell dimensions	a = 13.244(5) Å	α= 90°.
	b = 20.552(5) Å	β= 94.232(13)°.
	c = 25.657(5) Å	γ = 90°.
Volume	6965(3) $Å^3$	
Z	4	
Density (calculated)	1.291 Mg/m^3	
Absorption coefficient	0.095 mm^{-1}	
F(000)	2848	

View Article Online
DOI: 10.1039/C9NJ03254A

Crystal size	0.290 x 0.260 x 0.250 mm^3
Theta range for data collection	1.271 to 27.578°.
Index ranges	-17<=h<=16, -25<=k<=25, -33<=l<=32
Reflections collected	30731
Independent reflections	7642 [R(int) = 0.0785]
Completeness to theta = 25.242°	99.5 %
Refinement method	Full-matrix least-squares on F^2
Data / restraints / parameters	7642 / 4 / 456
Goodness-of-fit on F^2	1.064
Final R indices [I>2sigma(I)]	R1 = 0.0650, wR2 = 0.1784
R indices (all data)	R1 = 0.1058, wR2 = 0.1983
Extinction coefficient	none
Largest diff. peak and hole	0.381 and -0.484 $e.Å^{-3}$

Conclusion

In summary, very stable host-guest complexes have been isolated for the guest *N*,*N*′-bis[4-(dimethylaminophenyl)methyl]butane-1,4-diamine (**G**) and the cucuribit[*n*]urils Q[6] and Q[7]. The structures were verified by a range of methods including NMR spectroscopy, electronic adsorption, and ITC. The results revealed that for Q[6] a 1:1 host-guest complex is favoured which interestingly changes its mode of binding (from one of the aromatic motifs to the centre of G) over time (48h). For Q[7], a 2:1 host-guest complex is favoured, where the aromatic motifs are embedded in the Q[7] cavities. The single crystal X-ray structure clearly shows inclusion of the protonated guest molecule within the host Q[6] and it is localised therein by two N-H···O hydrogen bonds.

Experimental

All ^1H NMR spectra, including those for the titration experiments, were recorded at 20°C on a VARIAN INOVA-400 spectrometer. D_2O was used as a field-frequency lock, and the observed

View Article Online
DOI: 10.1039/C9NJ03254A

chemical shifts are reported in parts per million (ppm). Absorption spectra of the host-guest complexes were performed with an Aglient 8453 spectrophotometer at room temperature. The host and guests were dissolved in deionized water. UV-visible spectra was obtained at a concentration of 2.00-4.00×10^{-5} mol·L^{-1} guest and different Q[6] and Q[7] concentrations.

Starting materials and solvents for syntheses were purchased commercially and used as supplied without further purification. Q[6] and Q[7] were prepared and purified according to our previously published procedure. [7] The guest G was prepared by a modification of the procedure reported, [5] and is outline below. The association constants and thermodynamic parameters for the inclusion complexations of **G** with Q[6] and Q[7] were determined by titration calorimetry with an ITC instrument. The heat evolved was recorded at 298.15 K. An aqueous solution (0.1 mM) of either Q[6] or Q[7] was placed in the sample cell (1.3 mL). As a solution (1 mM) of the guest **G** was added in a series of 30 injections (10 μL). The heat of dilution was corrected by injecting the guest solution into deionized water and subtracting these data from those of the host−guest titration. Computer simulations (curve fitting) were performed using the Nano ITC analyze software.

Synthesis of N,N′-bis[4-(dimethylamino)phenyl]methyl-1,4-butanediamine (G).

A solution of 4-(dimethylamino)benzaldehyde (40 mmol) in ethanol (20 mL) was added to a stirred solution of 1, 4-butanediamine (15 mmol) in ethanol (20 mL), and the mixture was allowed to react at room temperature for 3 h. Thereafter, the resulting solution was filtered and then the white precipitate was washed with ethanol, and the solid material was re-dissolved in methanol (30 mL). The resulting solution was cooled in an ice bath and a solution of $NaBH_4$ (30

mmol) in methanol (20 mL) was added dropwise with stirring. On completion of the addition, the mixture was refluxed for 4 h. Some precipitate appeared, which was collected by filtration, concentrated HCl (10 mL) was then added to the filter mass. The chloride salt was precipitated from acetone, collected by filtration, washed with diethyl ether, and dried in air to give G. Yield: 47.8% ^{1}H NMR (400 MHz) δ 7.43 (d, *J* = 8.3 Hz, 4H), 7.33 (d, *J* = 8.3 Hz, 4H), 4.10 (s, 4H), 3.03 (s, 12H), 2.95 (t, 4H), 1.64 – 1.57 (m, 4H). ^{13}C NMR (101 MHz) δ 143.19, 132.70, 131.98, 121.18, 50.15, 46.63, 46.14, 22.83. Anal. Calcd. for $C_{22}H_{34}N_4$: C, 74.53; H, 9.67; N, 15.80; found C, 74.48; H, 9.74; N, 15.86.

*Synthesis of **1***

To a solution of *N*,*N*′-bis[4-(dimethylaminophenyl)methyl]butane-1,4-diamine (0.425 g, 0.001 mol) and $ZnCl_2$ (0.682 g, 0.005 mol) in 10 mL HCl (3M), Q[6] (0.996 mg, 0.001 mol) was added. The resulting reaction mixture was stirred for 5 min at 50°C and filtered. Slow solvent evaporation of the filtrate in air over a period of about three weeks provided rhombic colorless crystals of **1**. Yield: 12.4%.

Crystallography

A suitable colourless block was selected and this was mounted on a Bruker APEXII diffractometer. Data were collected in a series of phi and omega scans. The data were scaled and merged with SAINT (Bruker (2012). *SAINT*. Bruker AXS Inc., Madison, Wisconsin, USA) and corrected for the effects of absorption using SADABS (Bruker (2001). *SADABS*. Bruker AXS Inc., Madison, Wisconsin, USA). The structure was solved in I2/a using SHELXT. [8] All unique atoms were refined using anisotropic displacement parameters except those which are

View Article Online
DOI: 10.1039/C9NJ03254A

components of the minor disorder present. The disordered water present and chloride atoms that were not located in the difference plot were treated using SQUEEZE. [9]

Notes

CCDC 1935517 contains the supplementary crystallographic data for this paper and available free of charge from ccdc.cam.ac.uk

Acknowledgements

We thanks the National Natural Science Foundation of China (NSFC no 21861011), the Major Program for Creative Research Groups of Guizhou Provincial Education Department (2017-028), the Science and Technology Fund of Guizhou Province (No. 2016-1030, 2018-5781) and the Innovation Program for High-level Talents of Guizhou Province (No. 2016-5657) are gratefully acknowledged. CR thanks the EPSRC for an Overseas Travel Grant.

References

[1] (a) F. N. Meng, X. Y. Yao, Y. L. Ying, J. J. Zhang, H. Tian and Y. T. Long, *Chem. Commun.* **2015,** *51,* 1202–1205. (b) S. Dong, B. Zheng, F. Wang and F. Huang, *Acc. Chem. Res.* **2014,** *47,* 1982–1994. (c) Z. Xu, X. Lyu, B. Yang, W. Cao, R. Li, X. Zhang, X. Zhang, G. Fan, X. Kong, Q. Liu, *Colloid. Surface. A*, 2019, *569*, 28-34. (d) K. Jie, Y. Zhou, E. Li, F. Huang, *Acc. Chem. Res.* 2018, *51*, 2064-2072. (e) J. Zhou, G. Yu, F. Huang, *Chem. Soc. Rev.* 2017, *46*, 7021-7053. (f) N. Sun, X. Xiao, J. Jiang, *Advanced Science*, 2015, 2, 1500082. (g) H. Liu, Y. Ding, B. Yang, Z.

Liu, X. Zhang, Q. Liu, *ACS Sustainable Chem. Eng.*, 2018, *6*, 14383–14393. (h) Y. Zhou, K. Jie, F. Huang, *Chem. Commun.*, 2018, *54*, 12856-12859.

[2] (a) W. L. Mock, *Comp. Supramol. Chem*., **1996**, *2*, 477. (b) O. A. Gerasko, D. G. Samsonenko and V. P. Fedin, *Russ. Chem. Rev*., **2002**, *71*, 741. (c) K. Kim, *Chem. Soc. Rev*., **2002**, *31*, 96. (d) J. W. Lee, S. Samal, N. Selvapalam, H. -J. Kim and K. Kim, *Acc. Chem. Res*., **2003**, *36*, 621. (e) J. Lagona, P. Mukhopadhyay, S. Chak rabarti and L. Isaacs, *Angew. Chem., Int. Ed*., **2005**, *44*, 4844. (f) P. Montes-Navajas, M. González-Béjar, J. C. Scaiano and H. García, H. *Photochem. Photobiol. Sci.* **2009**, *8*, 1743–1747. (g) K. Wu, B. Yang, X. Zhu, W. Chen, X. Luo, Z. Liu, X. Zhang, Q. Liu , *New J. Chem.*, 2018,*42*, 18749-18758. (h) V. D. Uzunova, C. Cullinane, K. Brix, W. M. Nau and A. I. Day, *Org. Biomol. Chem*. **2010**, *8*, 2037–2042. (i) R. H. Gao, L. X. Chen, K. Chen, Z. Tao, X, Xiao, *Coordin. Chem. Rev.,* 2017, 348, 1-24. (j) K. I. Kuok, S. Li, I. W. Wyman, and R. Wang, *Ann. N.Y. Acad. Sci*. **2017**, *1398*, 108–119. (k) J. Lian, P. Liu, X. Li, B. Bian, X. Zhang, Z. Liu, X. Zhang, G. Fan, L. Gao, Q. Liu , Colloid. Surface. A, 2019, *565*, 1-7. (l) M. J. Webber and R. Langer, *Chem. Soc. Rev.* **2017**, *46*, 6600-6620. (m) X. Yang, W. Zhao, Z. Wang, Y. Huang, S. M. Y. Lee, Z. Tao, R. Wang, *Food and Chemical Toxicology*, **2017**, *108*, 510-518. (n) X. Zhang, X. Xu, S. Li, L. Wang, J. Zhang, R. Wang, *Scientific Reports*, **2018**, *8*, 8819. DOI:10.1039/b9pp00041k.

[3] W. J. Peveler, H. Jia, T. Jeen, K. Rees, T. J. Macdonald, Z. Xia, W. –I. K. Chio, S. Moorthy, I. P. Parkin, C. J Carmalt, W. R. Algar and T.-C. Lee, *Chem. Commun*. **2019**, *55*, 5495-5498.

View Article Online
DOI: 10.1039/C9NJ03254A

[4] (a) H. -B. Hou, Z. -Z. Gao, D. Bai, Z. Tao, T. J. Prior, C. Redshaw, X. Xiao, *Supramol. Chem*. **2017**, *9*, 680-685. (b) H. Feng, J. Kan, C. Redshaw, B. Bian, Z. Tao, X. Xiao, *Supramol. Chem.* **2019***, 4,* 260-267. (b) W. Xu, J. Kan, B. Yang, T. J. Prior, B. Bian, X. Xiao, Zhu Tao Carl Redshaw, *Chem. Asian J.*, 2019, *14*, 235-242. (c) Y. Xia, C. -Z. Wang, M. Tian, Z. Tao, X. –L. Ni, T. J. Prior, C. Redshaw. *Molecules*, **2018**, *23*, 175. (d) W. Xu; J. Kan; C. Redshaw; B. Bian; Y. Fan; Z. Tao, X. Xiao, *Supramol. Chem*. **2019**, *31*, 457-465. (f) X. Xiao，L. He，Z. Tao，S. Xue, Q. Zhu, A. Day, *Supramol. Chem*. **2010**, *22*, 194–201.

[5] X. Xiao, J. -X. Liu, Z. -F. Fan, K. Chen, Q. -J. Zhu, S. -F. Xue and Z. Tao, *Chem. Commun*. **2010**, *46*, 3741-3743.

[6] B. Chen and R. K. Mallampalli, Compositions and methods for treating diseases and conditions, US patent No. US2018134693 A1, May 17, 2018.

[7] (a) A. I. Day, A. P. Arnold, R. J. Blanch and B. Snushall, *J. Org. Chem.* **2001,** *66,* 8094–8100. (b) J. Kim, I. S. Jung, S. Y. Kim, E. Lee, J. K. Kang, S. Sakamoto, K. Yamaguchi and K. Kim, *J. Am. Chem. Soc*. **2000**, *122*, 540–541. (c) A. Day, A. P. Arnold, R. J. Blanch and B. Snushall, *J. Org. Chem*. **2001**, *66*, 8094–8100.

[8] G. M. Sheldrick, *Acta Cryst.* **2015**, *A71*, 3-8.

[9] A. L. Spek, *Acta Cryst.* **2015**, *C71*, 9-18.